Liquid Crystals
Publication details, including instructions for authors and subscription information:
http://www.informaworld.com/smpp/title~content=t713926090

Uniaxial and biaxial liquid crystal phases in colloidal dispersions of board-like particles

E. van den Pol[a]; D. M. E. Thies-Weesie[a]; A. V. Petukhov[a]; D. V. Byelov[a]; G. J. Vroege[a]
[a] Van't Hoff Laboratory for Physical and Colloid Chemistry, Debye Institute for Nanomaterials Science, Utrecht University, Padualaan 8, CH Utrecht, The Netherlands

Online publication date: 06 July 2010

To cite this Article van den Pol, E. , Thies-Weesie, D. M. E. , Petukhov, A. V. , Byelov, D. V. and Vroege, G. J.(2010) 'Uniaxial and biaxial liquid crystal phases in colloidal dispersions of board-like particles', Liquid Crystals, 37: 6, 641 — 651
To link to this Article: DOI: 10.1080/02678291003798164
URL: http://dx.doi.org/10.1080/02678291003798164

Liquid Crystals,
Vol. 37, Nos. 6–7, June–July 2010, 641–651

Taylor & Francis
Taylor & Francis Group

INVITED ARTICLE

Uniaxial and biaxial liquid crystal phases in colloidal dispersions of board-like particles

E. van den Pol, D.M.E. Thies–Weesie, A.V. Petukhov, D.V. Byelov and G.J. Vroege*

Van't Hoff Laboratory for Physical and Colloid Chemistry, Debye Institute for Nanomaterials Science, Utrecht University, Padualaan 8, 3584 CH Utrecht, The Netherlands

(*Received 8 December 2009; accepted 11 March 2010*)

Dispersions of board-like goethite (α-FeOOH) particles with short-range repulsive interaction form a versatile colloidal model system, showing a nematic, smectic A and columnar phase. In high magnetic fields a biaxial nematic phase is induced with the shortest dimension of the particles aligned along the field. Moreover, if particles have a shape almost exactly in between rod-like and plate-like they can spontaneously, without external magnetic field, form biaxial nematic and biaxial smectic A phases, which is in accordance with theoretical predictions. The macroscopic domains were oriented by a magnetic field and their structure was revealed by small-angle X-ray scattering. Our results suggest that biaxial phases can be readily obtained by a proper choice of the particle shape.

Keywords: mineral liquid crystals; biaxial phases; colloids; magnetic particles; X-ray scattering

1. Introduction

1.1 Biaxial phases

It is now 30 years since Yu and Saupe reported the first experimental observation of a biaxial nematic (N_B) phase, which was made in a micellar system [1]. The N_B phase is a modification of the usual (uniaxial) nematic (N_U) phase. In the N_U phase a spontaneous orientation of the main particle axis occurs: either along the particle's long axis in rod-like systems or along the particle's short axis in plate-like systems. Biaxiality occurs if particles also orient along a second axis perpendicular to their main orientation as shown in Figure 1(b) and (c). The N_B phase has potential advantages for use in electro-optical applications, such as flat-screen TV sets [2]. Currently, an N_U phase is used, which can be realigned using a small electric field. An N_B phase has the potential advantage that both molecular axes are aligned instead of one. If the long axis can be fixed, faster switching between different birefringent states is possible by rotating the short axes [3]. In this respect, a ferroelectric nematic liquid crystal can also be interesting, where the transverse dipoles of molecules can be aligned coherently to produce a large overall polarisation [4–6].

Freiser was the first to predict the existence of an N_B phase in 1970 [7], and a few years later theoretical phase diagrams were published [8, 9]. From then on, a large amount of theoretical work and many computer simulations have been devoted to the N_B phase [10–16]. A simulated phase diagram is shown in Figure 2 [11]. It has been shown that a biaxial phase is expected to be found for molecules with a shape exactly in between rod-like and plate-like, so when $L/W \simeq W/T$ (with L, W and T the length, width and thickness). A full phase diagram, including other (liquid) crystalline phases, was given by Taylor and Herzfeld and they found that the formation of a biaxial layer-like smectic phase strongly competes with the N_B phase [12]. Incorporating length polydispersity destabilises the smectic phase and might reduce this effect [13].

Another possible way to obtain a biaxial nematic phase is by using a mixture of rod-like and plate-like particles. This was already shown theoretically in 1973 [17] and has recently also been observed with computer simulations [18]. The difficulty here is the usually more favourable demixing into two uniaxial phases, one rich in rods and the other rich in plates [19–22].

For almost 40 years, there has been a search for biaxiality in liquid crystalline phases. The very few examples found so far are still debated and involve complicated interactions and complex (molecular) shapes [1, 2, 23–28]. For the classical lyotropic micellar system of Yu and Saupe [1] different suggestions have been raised about the nature of this biaxial phase. One difficulty is that micelles are adaptive systems where particle shape and phase symmetry mutually influence each other. At first it was thought that a mixture of rod-like and plate-like micelles induced the N_B phase, but later it was revealed that the micelles actually have a biaxial shape themselves [23]. It took until 2004 before seemingly conclusive evidence was found for the presence of an N_B phase in thermotropic liquid crystals [24, 25]. However, there is still an ongoing heated debate about this subject [2, 26–28], since it

*Corresponding author. Email: g.j.vroege@uu.nl

ISSN 0267-8292 print/ISSN 1366-5855 online

DOI: 10.1080/02678291003798164
http://www.informaworld.com

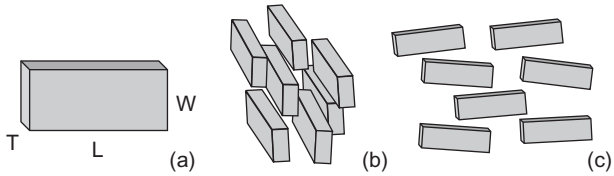

Figure 1. (a) Idealised shape of a goethite particle, (b) N_B phase oriented with the largest dimension (L) of the particles into the paper, (c) N_B phase oriented with the smallest dimension (T) of the particles into the paper.

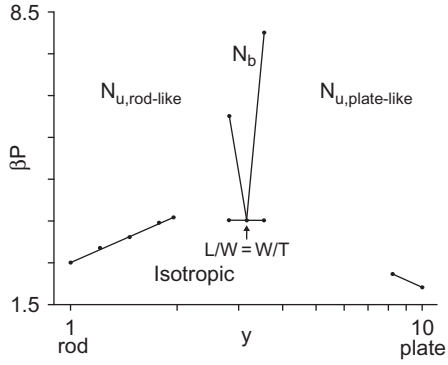

Figure 2. Simulated phase diagram of a hard fluid of biaxial ellipsoids, with $y = W/T$ and $L/T = 10$; redrawn from [11], with permission.

turns out to be very difficult to prove biaxiality. Recently, the existence of N_B phases in bent-core molecular systems was questioned again [29, 30]. In particular, it was suggested that the so-called biaxial nematic X-ray patterns are actually caused by smectic C type fluctuations in the nematic phase.

A biaxial smectic A (SmA_B) phase has been found for the first time in a side-chain polymer system that was aligned by a magnetic field [31]. Without alignment in an external field the phase was also found, for example by using bent-core molecules in an anisotropic medium [32] and in a binary mixture of a board-like metallomesogen with trinitrofluorenone [33].

1.2 Colloidal liquid crystals

Apart from the extensively studied molecular liquid crystals, anisometric colloids can also form liquid crystal phases when dispersed in a liquid [34–36]. These systems have some advantages, such as their enhanced susceptibility to external fields [37–41]. They are also less sensitive to temperature changes and have a good thermal stability. Furthermore, they can be very cheap because some of them can even be found in a natural form. As a model system these particles are interesting because of their relatively large size, tunable shape and adjustable interactions.

In such systems a perfect anchoring is usually difficult to realise, making it hard to obtain large domains of a certain orientation. For some colloidal particles the magnetic properties can be used to overcome this problem, since a small magnetic field can align the domains along the field direction.

Colloidal particles usually have a relatively high density, so that sedimentation effects play an important role in their phase behaviour [42]. Leaving these dispersions in a vertical position, a sedimentation equilibrium profile will form and a density gradient is observed. Furthermore, fractionation will occur in these inherently polydisperse systems. These factors make it possible to have several liquid crystal phases within one sample, as has been observed, for example, in gibbsite and goethite dispersions [43–45].

1.3 Colloidal biaxial phases

The examples of molecular biaxial phases mentioned previously have different types of interactions and either an ill-controlled or complex shape, making a comparison with theory rather difficult. Colloidal liquid crystalline particles are potentially interesting in this respect because they can be synthesised in different shapes and have short-range repulsive interactions. Although most attention has been paid to rod-like or plate-like particles, board-like colloids can also be obtained. These board-like particles are promising because – as we have indicated – theory and simulations suggest that a biaxial nematic phase can be formed if particles have dimensions $L/W \simeq W/T$ [8, 9, 11].

In colloidal systems a biaxial nematic gel state was observed for vanadium pentoxide [46]. These fairly rigid particles have a ribbon structure which is closely related to that of bulk crystalline (orthorhombic) V_2O_5 [47]. The ribbons are well-defined bilayers of single V_2O_5 layers made of square pyramidal VO_5 units. These slabs are separated by water molecules and stack along the z-axis of a monoclinic unit cell. Particles with dimensions $250 \times 25 \times 1$ nm were used to study the biaxiality of the nematic phase. A dispersion of these particles was studied in a Couette shear cell which produces an intrinsically biaxial shear. Small-angle X-ray scattering (SAXS) was used to study the organisation of the ribbons, by sending X-rays either radially, through the centre of the cell, or tangentially, through the gap between the cylinders. The combination of these two perpendicular cuts in reciprocal space provided a complete description of the symmetry of the structure. At volume fractions larger than 4% both configurations led to anisotropic SAXS patterns, which demonstrates the biaxial nematic symmetry. When the shear flow was stopped

the biaxial orientation did not relax within hours after stopping the shear. However, this nematic phase is a gel so the biaxial alignment of the ribbons may have been induced by the shear and then trapped in the gel.

Another good candidate to show a biaxial phase is goethite which is a versatile mineral liquid crystal, already known to form readily nematic, columnar and smectic phases [45, 48, 49]. These particles have a board-like shape (see Figure 1(a)) and by tuning the experimental conditions during synthesis we were able to make systems with a range of particle dimensions [50], one of them with $L/W = 3.1$ and $W/T = 3.0$. This is close to the condition $L/W \simeq W/T$ where biaxial phases are to be expected.

2. Experimental methods

2.1 Synthesis

Different synthesis methods were used to obtain systems with different polydispersities, as published earlier by Thies–Weesie *et al.* [50]. The systems with a high polydispersity (g55 and g35) were obtained by hydrolysis of iron nitrate at high pH according to Lemaire *et al.* [51]. 1 M NaOH (Acros, reagent ACS, pellets, 97+%) was added dropwise, with stirring, to a 0.1 M iron nitrate (Fisher Scientific, p.a.) solution until a pH of 11–12 was reached. The precipitate was aged for nine days after which the supernatant was removed and the sediment was washed two times with doubly distilled (dd) water and 3 M HNO_3 (Merck, p.a., 65%) to electrostatically charge the particles by proton adsorption. After centrifuging and redispersing in dd water three times, the particles were redispersed in dd water to obtain a stable dispersion in water at pH 3. To obtain a lower polydispersity (g35) more centrifugation steps were used.

The system with the lowest polydispersity (g17) was obtained by a slightly adjusted forced hydrolysis method as described by Krehula *et al.* [52]. 25 mL of 25% TMAH (tetramethyl ammonium hydroxide, Aldrich, 25% w/w in water) was added, under vigorous stirring, to a solution of 0.16 M iron nitrate. The solution was aged for 12 days at 100°C. The dispersion obtained was centrifuged and stabilised as described previously.

The biaxial system was obtained in almost the same way as the method first described. The aging time was 14 days and for centrifugation a larger volume was used [53].

It is assumed that after many centrifugation steps the salt concentration is determined by the H^+ and charge-compensating NO_3^- concentrations. The Debye length is then 10 nm at most.

2.2 Characterisation

Particle size distributions were determined by transmission electron microscopy (TEM) using a Technai 10 and 12 (FEI company) electron microscope. The particles have a more or less rectangular board-like shape with three different dimensions: length L, width W and thickness T. The lengths and widths of about 500 particles were measured with iTEM imaging software to determine the average length, $\langle L \rangle$, and width, $\langle W \rangle$, and their standard deviation δ_L and δ_W. The length polydispersity is then defined as $\sigma_L = \delta_L / \langle L \rangle$. Also correlations between the length and width were determined by measuring the length and width of each particle together. The thickness was determined separately and was more difficult to measure because not so many particles lay on their side on the TEM grid. Therefore, for most systems only about 20 particles thicknesses were measured, except for the biaxial system where we averaged over 150 particle thicknesses.

For some systems particle size distributions were also determined as a function of the height in the capillary. To this end, capillaries were cut into small pieces after first freezing them in liquid nitrogen. The pieces were put in small vials, after which water was added. The particles were homogeneously dispersed by ultrasonication and the different fractions were analyzed by TEM.

2.3 Small-angle X-ray scattering

Samples with different volume fractions were prepared in flat glass capillaries (Vitrocom RT3524) with internal dimensions of $0.2 \times 4.0 \times 100$ mm. The capillaries were closed with two-component epoxy glue (Bison Kombi rapide) and kept in a vertical position to allow the establishment of the sedimentation equilibrium profile. The samples of the g55 system were made in November 2003, those of g35 in January 2004 and those of g17 in December 2004. Of the biaxial system, Capillary 1 (initial volume fraction of 7.5%) was made in December 2004 and Capillary 2 (initial volume fraction of 10.6%) was made in January 2006. Due to slow evaporation the overall volume fractions had increased to 13.5% and 25.6%, respectively, at the time of the measurements.

To study the liquid crystalline phase behaviour, SAXS measurements were performed. For thermotropic systems the main technique to prove biaxiality is nuclear magnetic resonance, but this technique cannot be used here because the system is sensitive even to low magnetic fields and at fields above 250 mT the system changes dramatically (see Section 4). The SAXS measurements were performed at the BM26 DUBBLE beamline [54], using the microradian resolution setup

[55], and at the ID02 High Brilliance beamline of the European Synchrotron Radiation Facility (ESRF, Grenoble, France) [56]. A variable permanent magnet (from the ID02 beamline) was used, which could reach a magnetic field of up to 1.5 T. Two stacks of NdFeB permanent magnets generated the field and the distance between them could be adjusted to reach the desired field strength. Different stacks were available, one set giving a field perpendicular to the X-ray beam and another set a field parallel to the X-ray beam. So, by changing the stacks the direction of the magnetic field could also be altered.

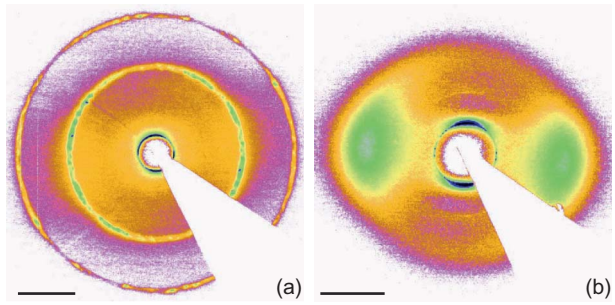

Figure 3. (a) SAXS pattern showing a coexisting smectic A and columnar phase (g35), (b) SAXS pattern of a single smectic A phase (g17). The scale bars are 0.05 nm^{-1}.

3. General phase behaviour of goethite

To investigate the general phase behaviour of goethite, several dispersions have been studied extensively by SAXS [57]. The particle dimensions of the systems studied (g17, g35 and g55) are shown in Table 1. All these dispersions have $L/W > W/T$ and form a nematic phase which is uniaxial. Recently, it was shown that goethite particles can also form a smectic phase, even in a highly (over 50%) polydisperse system [45]. Because of the possibility of creating dispersions with different polydispersities [50], it was possible to study the effect of polydispersity on the phase behaviour of goethite in detail [57]. It was found that the systems with a high polydispersity (g55 and g35) form an isotropic (I), nematic (N), smectic A (SmA) and columnar (C) phase. A SAXS pattern of a coexisting SmA and C phase is shown in Figure 3(a). The sharp scattering peaks at a small angle correspond to the smectic periodicity and the broad scattering peaks, originating from the liquid-like interactions within the smectic layers, can be seen under the sharper columnar peaks around $q = 0.08$ nm^{-1}. The columnar phase is recognised by the powder-like sharp scattering rings. These sharp peaks originate from a centred rectangular structure (*c2mm* symmetry group) [49]. The system with a lower polydispersity (g17) also shows a smectic phase, but does not show a columnar phase (Figure 3(b)).

The occurrence of a smectic phase in a system with such a high polydispersity is surprising, because the polydispersity is expected to suppress the formation of ordered phases [58, 59]. It was shown by computer simulations on hard spherocylinders, in the limit of infinite aspect ratio, that a smectic phase can only form if the length polydispersity is below 18% [60]. Above this terminal polydispersity a columnar phase rather than a smectic phase is expected at high volume fractions. A columnar phase can accommodate broader length distributions because particles do not have to fit into layers.

To study this in more detail, TEM was used to determine particle size distributions as a function of the height in the capillary and in this way the real particle distributions at different heights in different phases could be determined. The length distribution of fractions at different heights in a sample of g55 are shown in Figure 4; f10 is at the top of the capillary and f1 at the bottom. It can be seen that the average length drastically increases towards the bottom of the capillary, indicating fractionation during sedimentation. Furthermore, the distribution of the pure smectic part (f3) is the narrowest, although it still contains some shorter particles. It can be seen that the largest difference between the pure smectic phase and the coexisting smectic and columnar phase (f1) is in the

Table 1. Goethite particle dimensions

System	$\langle L \rangle$ (nm)	σ_L (%)	$\langle W \rangle$ (nm)	σ_W (%)	$\langle T \rangle$ (nm)	$\langle L \rangle / \langle W \rangle$	$\langle W \rangle / \langle T \rangle$
g55	216	55	35	48	~16	6.2	2.2
g35	282	35	68	32	~25	4.1	2.7
g17	220	17	62	29	~23	3.5	2.7
biaxial	254	25	83	25	28	3.1	3.0

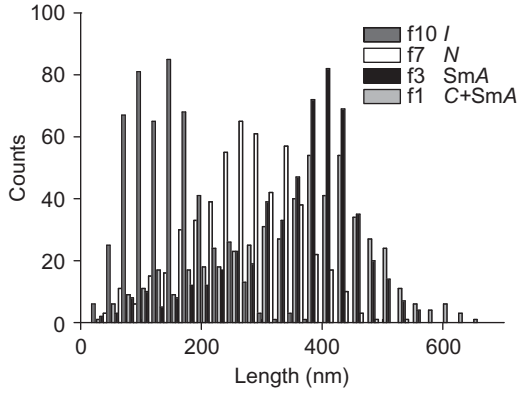

Figure 4. Length distributions of the fractions f1 (C+SmA), f3 (SmA), f7 (N) and f10 (I) of the g55 system.

presence of very long (~600 nm) particles in the latter phase. Presumably, these large particles cannot fit into the smectic layers but can be accommodated in the columnar phase.

4. Magnetic properties and induced biaxiality

Besides their rich liquid crystalline phase behaviour, goethite particles also have peculiar magnetic properties. Special magneto-optical effects of aqueous colloidal suspensions of mixed iron oxides were recognised by Majorana in 1902 [37] and further studied by Cotton and Mouton in 1907 [38]. It turned out that one of the components in their samples was goethite.

Bulk goethite is antiferromagnetic. The structure consists of double chains of octahedra occupied by iron atoms. Within a chain their spins are parallel, but there is an antiferromagnetic coupling between neighbouring chains. The Néel temperature depends on the size of the particles and varies between 325 and 400 K [51]. The magnetic easy axis of the magnetic susceptibility tensor $\boldsymbol{\chi}$ lies along the shortest particle dimension. Moreover, goethite nanorods also have a weak permanent magnetic moment $\boldsymbol{\mu}$ along the long axis of the particles. This is presumably caused by non-compensated surface spins. The magnetic energy per particle in a magnetic field, **B**, is given by [51]

$$E_m = -\boldsymbol{\mu} \cdot \mathrm{B} - \frac{V}{2\mu_0} \mathrm{B} \cdot \boldsymbol{\chi} \cdot \mathrm{B}, \qquad (1)$$

with V the particle volume [51]. The first term is the interaction between the particle dipole and the field and the second term is due to the induced magnetisation.

In a small field, the first term dominates, which has a minimum when the particles are aligned along the field. In contrast, the second term dominates at large fields when the energy reaches its minimum when the particles are aligned perpendicular to the field. Therefore, particles will align parallel to a small magnetic field, but perpendicular to a large magnetic field ($>$ 300 mT).

These goethite particles have a Frederiks transition at very low fields. Samples held in 20 μm thick flat capillaries aligned beyond a field threshold of only 20 $\pm$ 5 mT [48]. This field intensity is 50 times lower than expected for tobacco mosaic virus (TMV) [61] or in V_2O_5 suspensions [39]. It is about 25 times lower than is observed for usual thermotropic liquid crystals [62].

It was found that in high magnetic fields, when the particles are oriented perpendicular to the field, the nematic phase actually becomes biaxial [63]. This was found by birefringence measurements starting with a homeotropically aligned nematic sample. A field above the reorientation threshold was applied within the plane of the capillary. Large homeotropic domains grew and they displayed a weak birefringence that increased with the field intensity. If the nematic phase is uniaxial there should be no birefringence, which implies that this nematic phase is biaxial. It was shown that the thinnest dimension of the particles aligns along the field. This reveals that the main component of $\boldsymbol{\chi}$ in Equation (1) is along the particle short axis.

The induced biaxial nematic phase was also observed with SAXS [64]. Going from a small to a large magnetic field, not only did the peak orientations change by 90° because of particle reorientation, but the peak positions also changed. The liquid-like nematic peaks shifted to a larger angle (from 0.069 nm^{-1} to 0.086 nm^{-1}) going from a small to a large magnetic field (see Figure 5). This indicates smaller distances in the direction of the field compared to the distances found for the uniaxial nematic phase in a small field. This confirms that the smallest dimension of the particles aligns along the field in large magnetic fields and the phase is biaxial.

5. Biaxial correlations

Because of their board-like shape, goethite particles are potential candidates to form biaxial phases even without an external magnetic field. One of the systems that has dimensions coming close to $L/W \simeq W/T$, when a biaxial nematic phase would be expected, was described in Section 3 (g35, see Table 1). The actual ratios are $L/W = 4.1$ and $W/T = 2.7$. This system has been studied in detail with SAXS.

Signs of possible biaxiality were found in the scattering patterns when the sample was 4.5 years old. SAXS patterns are given at different heights in the capillary, from 2–5 mm from the bottom of the capillary (see Figure 6). In the lowest pattern sharp peaks can be observed originating from a columnar phase.

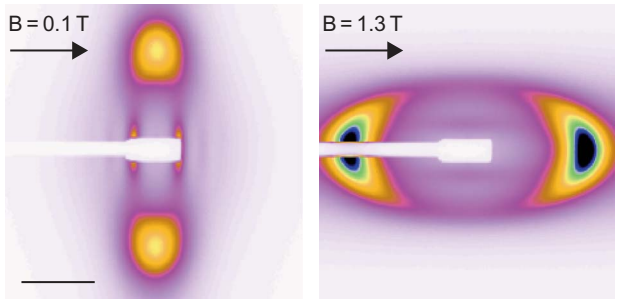

Figure 5. SAXS patterns of the nematic phase of goethite in a magnetic field. The scale bar is 0.05 nm^{-1}.

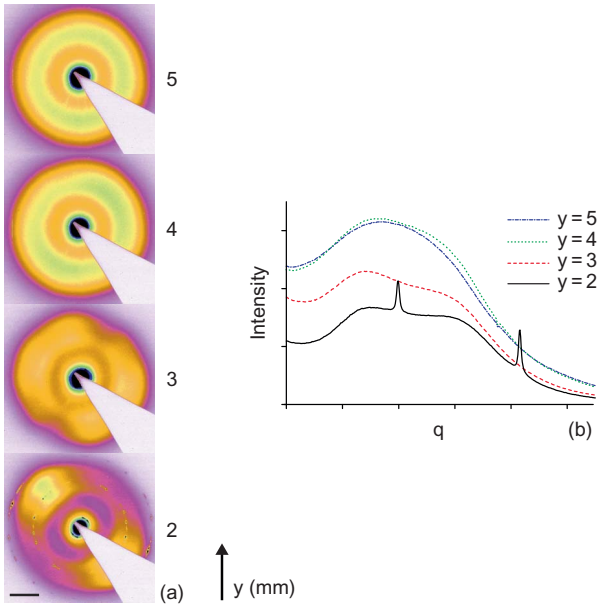

Figure 6. (a) SAXS patterns at different heights of a sample of the g35 system, with (b) the corresponding peak profiles. The scale bar is 0.05 nm^{-1}.

The broad peaks arise from the liquid-like interactions in the nematic phase.

In the lower part of the nematic phase double-peaked scattering can be seen, which is clearer in the peak profiles shown in Figure 6(b). Going up in the nematic phase the double peaks vanish and single peaks are observed. These double peaks can be an indication of biaxiality because they indicate two typical correlation distances, probably from the width and the thickness of the particles.

To check the biaxiality the sample was placed in a small magnetic field (25 mT) which was oriented along the X-ray beam. In that way the particles aligned along the field and also along the X-ray beam. If the nematic phase was really biaxial an anisotropic scattering pattern should be observed with two peaks at a different angle which are perpendicular to each other. This is because the width and thickness correlations should give a peak in orthogonal directions and at a different scattering angle. When we placed this sample in the field it showed the pattern displayed in Figure 7(b); the original pattern, without the magnetic field, is shown in Figure 7(a). It can be seen that the pattern actually becomes more isotropic when the field is applied. This implies that the nematic phase is not biaxial as a whole, but that it probably has some biaxial correlations on a local scale.

The g17 system seems to be closer to the biaxial condition $L/W \simeq W/T$ (see Table 1), but we did not find any double peaks in the nematic phase of this system. There can be different reasons for this. First, these samples had been standing for a shorter time before the SAXS measurements were carried out and in the other system it took years before the signs of biaxial correlations were observed. Furthermore, in these systems the thickness of only 20 particles could be measured (see Section 2.2), so there is a large error in the average thickness, giving also a large error in the W/T ratio.

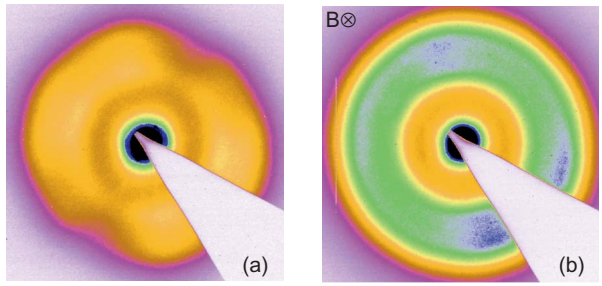

Figure 7. SAXS pattern of the nematic phase without magnetic field (a) and in a magnetic field of 25 mT, along the X-ray beam (b).

6. Biaxial nematic phase

Another system that has been studied has particles with average dimensions of $L \times W \times T = 254 \times 83 \times 28$ nm, with a polydispersity of 20–25% in all directions (see Table 1 and Figure 8) [53]. This gives $L/W = 3.1$ and $W/T = 3.0$ which is promising in view of finding an N_B phase. A schematic picture of the samples studied is given in Figure 9 together with a polarisation microscopy

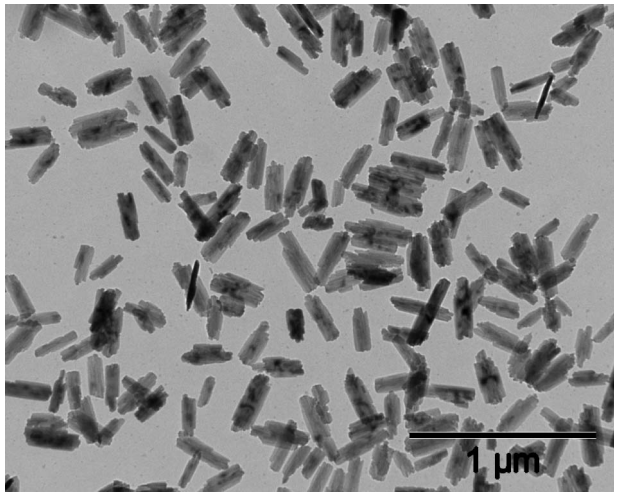

Figure 8. TEM picture of the goethite particles with $L/W \simeq W/T$.

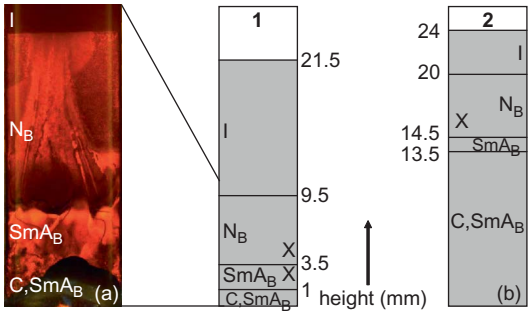

Figure 9. (a) Polarisation microscopy picture of Capillary 1. (b) Schematic picture of the measured capillaries described in Sections 6 and 7, indicating the isotropic (I), biaxial nematic (N_B), biaxial smectic (SmA_B) and the combination of columnar and smectic (C,SmA_B) phase. The x's correspond to the measurement positions discussed in this article.

picture. Because of sedimentation a concentration profile developed and several liquid crystalline phases could be observed in one capillary. SAXS was used together with a small external magnetic field to determine the phases present in the system.

Capillary 1 was first studied with the field aligned along the X-ray beam, so perpendicular to the paper. The magnetic poles were at maximum distance and gave a very small field of 3 mT. The SAXS pattern of the nematic phase is shown in Figure 10(a). It is clear that the pattern is now anisotropic, which is different from the system described in the previous section (see Figure 7(b)). Two orthogonal peaks at larger angles were observed corresponding to the width and thickness correlations; for the peak profiles in the horizontal (solid line) and vertical (dashed line) directions see Figure 10(d). In addition to the radial profiles, the azimuthal profiles of the scattering intensity along the circles at q values corresponding to the three main correlation peaks are shown in Figure 11(a). The q values chosen are illustrated by circles in the scattering patterns. One can clearly see that different positional correlation peaks appear along directions orthogonal to each other. The fact that the peaks are perpendicular to each other indicates that the particles are orientationally ordered in three directions, as is illustrated in Figure 1(b). This phase is clearly an N_B phase. It is also evident that an external field as low as 3 mT is sufficient to orient the particles along the field because no peak was observed at a small angle corresponding to the length correlations.

Increasing the field to 40 mT (see Figures 10(b), (e) and 11(b)) the only change was a higher intensity of the peaks. This indicates that the particles were better aligned at this field strength. Subsequently, the field direction was changed from parallel to perpendicular to the X-ray beam by replacing the magnetic poles. After applying again a magnetic field of 40 mT, peaks at small angles emerged in the field direction corresponding to correlations between the long axes of the particles (see Figures 10(c), (f) and 11(c)). The width correlations can now be seen in the vertical direction. In the same direction but at a larger angle there also appeared weak scattering corresponding to the thickness, presumably originating from a differently oriented domain caused by the reorientation process. The N_B phase changed orientation with the change of the magnetic field direction and was then predominantly like the

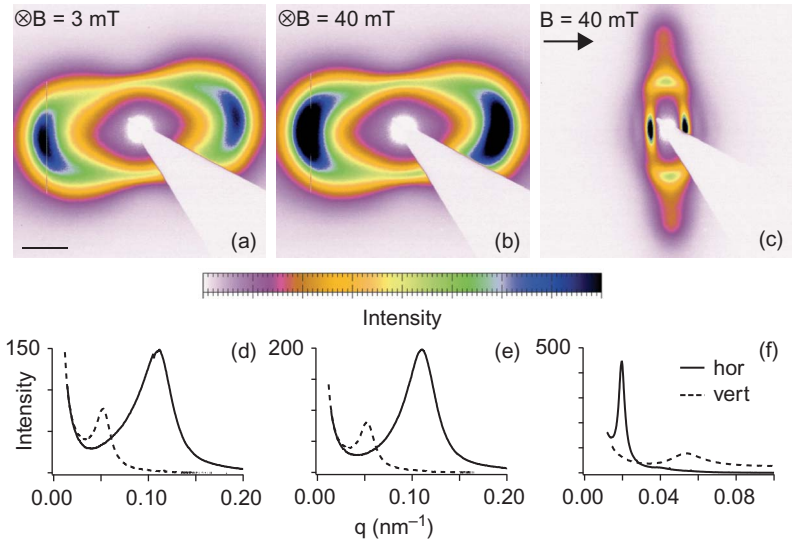

Figure 10. SAXS patterns of the N_B phase in Capillary 1 in a small magnetic field of (a) 3 mT and (b) 40 mT parallel (⊗) to the X-ray beam, and (c) of 40 mT perpendicular (→) to the X-ray beam, with the intensity profiles of a (d), b (e) and c (f) in the horizontal (solid line) and vertical (dashed line) directions. The scale bar is 0.05 nm^{-1}.

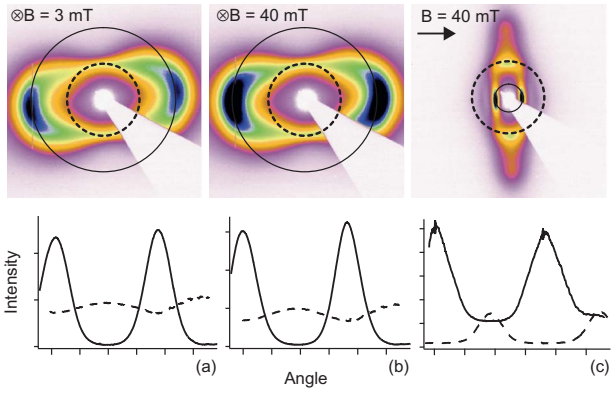

Figure 11. Plots of the intensity as a function of the angle at different q values of the SAXS patterns shown in Figure 10.

situation depicted in Figure 1(c). Table 2 summarises the positions and the radial widths of the liquid-like correlation peaks in Figure 10(e) and (f). One can see that the width of all the peaks, including that in the horizontal direction in Figure 10(f), is well beyond the instrument resolution, which was about 3×10^{-4} nm^{-1}. The normalised peak widths δ_q/q_0 are also comparable for the peaks originating from liquid-like interparticle correlations in the three orthogonal directions, which confirms the nematic nature of the phase.

Distances, d, were calculated from the scattering vector, q, of the three orthogonal peaks, observed in the scattering patterns measured with the different orientations of the magnetic field, from $d \approx 2\pi/q$. Ensemble-averaged distances d_L, d_W and d_T were found to be 320, 120 and 58 nm, which are slightly larger than the particle dimensions L, W and T of 254, 83 and 28 nm. The electric double layer around the charged particles is at least of the order of the Debye length (10 nm at most in this case). Taking this into account brings the dimensions close to the distances measured. Furthermore, polydispersity causes fractionation in the system and therefore mainly the longer particles are expected to be in the lower part of the capillary (where these measurements were carried out, see Figure 9) [57]. The measured d_L/d_W and d_W/d_T ratios are 2.7 and 2.1, while the actual particle ratios are $L/W = 3.1$ and $W/T = 3.0$. However, including the Debye length gives $L_{\text{eff}}/W_{\text{eff}} = 2.7$ and $W_{\text{eff}}/T_{\text{eff}} = 2.1$,

Table 2. Position q_0 and radial width δ_q of the peaks seen in Figure 10(e),(f).

		q_0/nm^{-1}	δ_q/nm^{-1}	δ_q/q_0
Figure 10(e)	vert	0.052	0.016	0.30
	hor	0.109	0.045	0.41
Figure 10(f)	vert	0.054	0.020	0.37
	hor	0.0195	0.0034	0.18

which now correspond well to the peak ratios measured. Together with the SAXS patterns these values give convincing evidence that an N_B phase was indeed found.

To be sure that the N_B phase is not field induced, measurements were performed without any magnetic field. Therefore, Capillary 2 (see Figure 9) was used, which had not been in a magnetic field before, and was first studied without any field. The observed SAXS pattern of the nematic phase is presented in Figure 12(a). It shows peaks at a small angle corresponding to the length correlations and perpendicular to that peaks at a larger angle from the width correlations. No peak is observed at a larger angle which would correspond to distances of the order of the thickness of the particles. This implies that the smallest dimension of the particles is aligned along the X-ray beam and that the three different dimensions of the particles are oriented orthogonal to each other. It is concluded that an N_B phase was also present in zero field and is not induced by the magnetic field. Furthermore, the domain of the N_B phase is larger than the X-ray beam, which is about 0.5–1 mm in diameter at the sample position.

At 40 mT, the N_B phase aligned along the field as was observed before (see Figure 12b). After the field was reduced to 3 mT for one hour, it was seen that the N_B phase slowly relaxed into the direction of its original orientation (Figure 12(c)).

Interestingly, a direct transition from the I to the N_B phase was observed in both capillaries without an N_U phase in between. An intermediate N_U phase is expected if the L/W and W/T ratios are slightly different (see Figure 2) [8–11]. It might be that polydispersity has a stabilising effect on the N_B phase compared to the N_U phase, which has been shown to be the case for the N_U phase compared to the I phase [65–67]. Another aspect can be a possible electrostatic heterogeneity of the particles.

We attempted to perform additional birefringence measurements on the N_B phase. Therefore, we tried to align the particles along the optical axis, using a small field along this optical axis, to obtain a homeotropic sample. The measured birefringence could then be compared with values measured for the induced

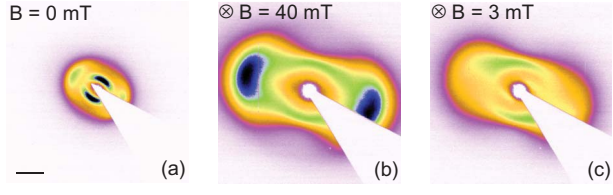

Figure 12. SAXS patterns of (a) the N_B phase in Capillary 2 in 0 mT, (b) in 40 mT (parallel ⊗ to the X-ray beam) and (c) the relaxation of the N_B phase shown at 3 mT. The scale bar is 0.05 nm^{-1}.

biaxial phase of goethite [63]. Unfortunately, the capillaries used (0.2 × 4.0 × 100 mm) were too thick to be able to observe anything optically. The problem is that goethite is a pigment and absorbs a lot of light. Further attempts will be made using thinner capillaries, but they will need time to equilibrate.

7. Biaxial smectic A phase

An SmA phase was also found in the same system. The same measurements were carried out for this phase, using Capillary 1. It did not align along the field of 3 mT (parallel to the X-ray beam, which is perpendicular to the paper), as can be seen from the small-angle peaks originating from the length correlations (see Figure 13(a)). The pattern is similar to that observed for the N_B phase in zero field (see Figure 12(a)), but with much sharper small-angle peaks. These very sharp and intense peaks, oversaturated in this picture, are characteristic of the periodicity of the smectic phase. Perpendicular to them, at larger angles, liquid-like peaks were observed corresponding to distances comparable to the width of the particles. However, no peaks were observed at even larger angles, so the smallest dimension of the particles was oriented along the X-ray beam. This implies that again the three different dimensions of the particles were oriented orthogonally to each other and an SmA_B phase was observed (see Figure 13(d)).

By increasing the field to 40 mT, peaks appeared at larger angles, while the peaks at small angles vanished (see Figure 13(b)). The observed SAXS pattern was then similar to the aligned N_B phase (see Figure 10(a),(b)), indicating that the smectic phase was now also aligned along the field and the widths and thicknesses of the particles were perpendicular to the field and perpendicular to each other. This shows that clearly the smectic phase is also biaxial. After rotating the field direction from parallel to perpendicular to the X-ray beam, sharp peaks from the length correlations (oversaturated in this picture) returned at small angles (Figure 13(c)). Second-order peaks were observed (Figure 13(c), zoom), suggesting a well-aligned smectic phase. The distances corresponding to the three different peak angles were calculated from the different SAXS patterns and found to be $d_L = 327$ nm, $d_W = 120$ nm and $d_T = 56$ nm, which are comparable to the distances found in the N_B phase. The d_L/d_W and d_W/d_T ratios measured are again 2.7 and 2.1.

Finally, we would like to stress that the observed biaxiality cannot be induced by artefacts such as anchoring at the capillary walls. The results shown in Figures 10(a),(b), 13(b) and 12(b) are obtained from domains with the particle's long axis normal to the capillary walls. In that case there can be no (biaxial) anchoring effect of the capillary walls. Moreover, the biaxiality is not induced by the magnetic field since the biaxial structure was also observed without applying a magnetic field and it remains after removal of the field.

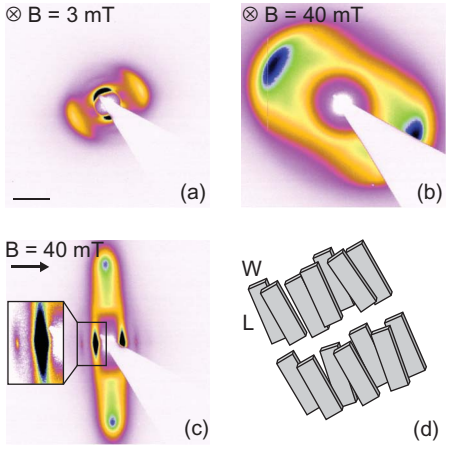

Figure 13. SAXS patterns of the SmA_B phase in Capillary 1 in a small magnetic field of (a) 3 mT and (b) 40 mT parallel (⊗) to the X-ray beam, and (c) of 40 mT perpendicular (→) to the X-ray beam (including zoom). The scale bar is 0.05 nm^{-1}. (d) The structure of the biaxial smectic phase, corresponding to (a).

8. Conclusions

Colloidal goethite dispersions form nematic, smectic and columnar phases. Even in systems with a high polydispersity a smectic phase can be observed because of sedimentation and fractionation. Furthermore, they have special magnetic properties causing them to align parallel to a small magnetic field and perpendicular to a large magnetic field. In high fields even a biaxial nematic phase is induced.

Without a magnetic field, in goethite dispersions with particle ratios L/W larger than W/T by at least a factor of 1.3, some biaxial correlations have been observed in one system but no real biaxial phase. However, in a dispersion of particles with $L/W \simeq W/T$ we clearly show the existence of biaxial nematic and biaxial smectic A phases. The magnetic properties of the particles have been used to align the domains in different directions during SAXS measurements, which allowed the construction of a complete picture of the biaxial phases. The macroscopically large domains are also observed without alignment by a magnetic field. Surprisingly, the N_B phase is stable over a large concentration range and no N_U phase was found. These results suggest that the biaxial nematic and biaxial smectic phases can be readily obtained by a proper choice of the particle dimensions, which for the first time confirms earlier theoretical work. Compared to the beautiful work of Yu and Saupe [1],

our particles have a fixed and well-defined shape. This system can be a model for smaller nanoparticles that could be useful for applications.

Acknowledgements

This work is part of the research program SFB TR6 of the 'Stichting voor Fundamenteel Onderzoek der Materie (FOM)', which is financially supported by the 'Nederlandse Organisatie voor Wetenschappelijk Onderzoek (NWO)' and 'Deutsche Forschungsgemeinschaft (DFG)'. The work of D.M.E. Thies–Weesie was performed as part of a NWO–CW TOP project. We thank P. Davidson for enlightening discussions and for his help, together with I. Dozov, with the birefringence measurements. We also thank the staff of the BM26 and ID02 beamlines of the ESRF for their excellent support and Th. Narayanan for sharing the magnet.

References

[1] Yu, L.J.; Saupe, A. *Phys. Rev. Lett.* **1980**, *45* (12), 1000.
[2] Luckhurst, G.R. *Nature* **2004**, *430* (6998), 413–414.
[3] Lee, J.H.; Lim, T.K.; Kim, W.T.; Jin, J.I. *J. Appl. Phys.* **2007**, *101* (3), 34105.
[4] Blinov, L.M. *Liq. Cryst.* **1998**, *24*, 143–152.
[5] Watanabe, T.; Miyata, S.; Furukawa, T.; Takezoe, H.; Nishi, T.; Sone, M.; Migita, A.; Watanabe, J. *Jpn. J. Appl. Phys. Part 2* **1996**, *35* (4B), 505–507.
[6] Francescangeli, O.; Stanic, V.; Torgova, S.I.; Strigazzi, A.; Scaramuzza, N.; Ferrero, C.; Dolbnya, I.P.; Weiss, T.M.; Berardi, R.; Muccioli, L.; Orlandi, S.; Zannoni, C. *Adv. Funct. Mater.* **2009**, *19* (16), 2592–2600.
[7] Freiser, M.J. *Phys. Rev. Lett.* **1970**, *24* (19), 1041.
[8] Alben, R. *Phys. Rev. Lett.* **1973**, *30* (17), 778.
[9] Straley, J.P. *Phys. Rev. A: At., Mol., Opt. Phys.* **1974**, *10* (5), 1881.
[10] Biscarini, F.; Chiccoli, C.; Pasini, P.; Semeria, F.; Zannoni, C. *Phys. Rev. Lett.* **1995**, *75* (9), 1803.
[11] Camp, P.J.; Allen, M.P. *J. Chem. Phys.* **1997**, *106* (16), 6681–6688.
[12] Taylor, M.P.; Herzfeld, J. *Phys. Rev. A: At., Mol., Opt. Phys.* **1991**, *44* (6), 3742.
[13] Vanakaras, A.G.; Bates, M.A.; Photinos, D.J. *Phys. Chem. Chem. Phys.* **2003**, *5* (17), 3700–3706.
[14] Care, C.M.; Cleaver, D.J. *Rep. Prog. Phys.* **2005**, *68* (11), 2665–2700.
[15] McBride, C.; Lomba, E. *Fluid Phase Equilib.* **2007**, *255* (1), 37–45.
[16] Berardi, R.; Muccioli, L.; Orlandi, S.; Ricci, M.; Zannoni, C. *J. Phys. Condens. Matter* **2008**, *20* (46), 463101.
[17] Alben, R. *J. Chem. Phys.* **1973**, *59* (8), 4299–4304.
[18] Cuetos, A.; Galindo, A.; Jackson, G. *Phys. Rev. Lett.* **2008**, *101* (23), 237802.
[19] Stroobants, A.; Lekkerkerker, H.N.W. *J. Phys. Chem.* **1984**, *88* (16), 3669–3674.
[20] Camp, P.J.; Allen, M.P.; Bolhuis, P.G.; Frenkel, D. *J. Chem. Phys.* **1997**, *106* (22), 9270–9275.
[21] Wensink, H.H.; Vroege, G.J.; Lekkerkerker, H.N.W. *Phys. Rev. E: Stat., Nonlinear, Soft Matter Phys.* **2002**, *66* (4), 41704.
[22] Varga, S.; Galindo, A.; Jackson, G. *Phys. Rev. E: Stat., Nonlinear, Soft Matter Phys.* **2002**, *66* (1), 11707.
[23] Galerne, Y.; Figueiredo Neto, A.M.; Liebert, L. *J. Chem. Phys.* **1987**, *87* (3), 1851–1856.
[24] Madsen, L.A.; Dingemans, T.J.; Nakata, M.; Samulski, E.T. *Phys. Rev. Lett.* **2004**, *92* (14), 145505.
[25] Acharya, B.R.; Primak, A.; Kumar, S. *Phys. Rev. Lett.* **2004**, *92* (14), 145506.
[26] Luckhurst, G.R. *Thin Solid Films* **2001**, *393* (1–2), 40–52.
[27] Galerne, Y. *Phys. Rev. Lett.* **2006**, *96* (21), 219803.
[28] Madsen, L.A.; Dingemans, T.J.; Nakata, M.; Samulski, E.T. *Phys. Rev. Lett.* **2006**, *96* (21), 219804.
[29] Van Le, K.; Mathews, M.; Chambers, M.; Harden, J.; Li, Q.; Takezoe, H.; Jákli, A. *Phys. Rev. E: Stat., Nonlinear, Soft Matter Phys.* **2009**, *79* (3), 30701.
[30] Vaupotic, N.; Szydlowska, J.; Salamonczyk, M.; Kovarova, A.; Svoboda, J.; Osipov, M.; Pociecha, D.; Gorecka, E. *Phys. Rev. E: Stat., Nonlinear, Soft Matter Phys.* **2009**, *80* (3), 30701.
[31] Leube, H.F.; Finkelmann, H. *Makromol. Chem.* **1991**, *192* (6), 1317–1328.
[32] Pratibha, R.; Madhusudana, N.V.; Sadashiva, B.K. *Science* **2000**, *288* (5474), 2184–2187.
[33] Hegmann, T.; Kain, J.; Diele, S.; Pelzl, G.; Tschierske, C. *Angew. Chem.* **2001**, *113* (5), 911–914.
[34] Sonin, A.S. *J. Mater. Chem.* **1998**, *8* (12), 2557–2574.
[35] Gabriel, J.C.P.; Davidson, P. *Adv. Mater.* **2000**, *12* (1), 9–20.
[36] Davidson, P.; Gabriel, J.C.P. *Curr. Opin. Colloid Interface Sci.* **2005**, *9*, 377–383.
[37] Majorana, Q. *Rend. Accad. Lincei* **1902**, *11–1*, 374.
[38] Cotton, A.; Mouton, H. *Ann. Chim. Phys.* **1907**, *11*, 145.
[39] Commeinhes, X.; Davidson, P.; Bourgaux, C.; Livage, J. *Adv. Mater.* **1997**, *9* (11), 900–903.
[40] van der Beek, D.; Petukhov, A.V.; Davidson, P.; Ferre, J.; Jamet, J.P.; Wensink, H.H.; Vroege, G.J.; Bras, W.; Lekkerkerker, H.N.W. *Phys. Rev. E: Stat., Nonlinear, Soft Matter Phys.* **2006**, *73* (4), 41402.
[41] Michot, L.J.; Bihannic, I.; Maddi, S.; Funari, S.S.; Baravian, C.; Levitz, P.; Davidson, P. *Proc. Natl. Acad. Sci.* **2006**, *103* (44), 16101–16104.
[42] Wensink, H.H.; Lekkerkerker, H.N.W. *Europhys. Lett.* **2004**, *66* (1), 125–131.
[43] van der Kooij, F.M.; Kassapidou, K.; Lekkerkerker, H.N.W. *Nature* **2000**, *406*, 868–871.
[44] van der Kooij, F.M.; Vogel, M.; Lekkerkerker, H.N.W. *Phys. Rev. E: Stat., Nonlinear, Soft Matter Phys.* **2000**, *62* (4), 5397–5402.
[45] Vroege, G.J.; Thies-Weesie, D.M.E.; Petukhov, A.V.; Lemaire, B.J.; Davidson, P. *Adv. Mater.* **2006**, *18*, 2565–2568.
[46] Pelletier, O.; Bourgaux, C.; Diat, O.; Davidson, P.; Livage, J. *Eur. Phys. J. B* **1999**, *12* (4), 541–546.
[47] Petkov, V.; Trikalitis, P.N.; Bozin, E.S.; Billinge, S.J.L.; Vogt, T.; Kanatzidis, M.G. *J. Am. Chem. Soc.* **2002**, *124* (34), 10157–10162.
[48] Lemaire, B.J.; Davidson, P.; Ferré, J.; Jamet, J.P.; Panine, P.; Dozov, I.; Jolivet, J.P. *Phys. Rev. Lett.* **2002**, *88* (12), 125507.
[49] Lemaire, B.J.; Davidson, P.; Panine, P.; Jolivet, J.P. *Phys. Rev. Lett.* **2004**, *93*, 267801.
[50] Thies-Weesie, D.M.E.; de Hoog, J.P.; Hernandez Mendiola, M.H.; Petukhov, A.V.; Vroege, G.J. *Chem. Mater.* **2007**, *19*, 5538–5546.
[51] Lemaire, B.J.; Davidson, P.; Ferré, J.; Jamet, J.P.; Petermann, D.; Panine, P.; Dozov, I.; Jolivet, J.P. *Eur. Phys. J. E* **2004**, *13*, 291–308.

[52] Krehula, S.; Popović, S.; Musić, S. *Mater. Lett.* **2002**, *54*, 108–113.
[53] van den Pol, E.; Petukhov, A.V.; Thies-Weesie, D.M.E.; Byelov, D.V.; Vroege, G.J. *Phys. Rev. Lett.* **2009**, *103* (25), 258301.
[54] Bras, W.; Dolbnya, I.P.; Detollenaere, D.; van Tol, R.; Malfois, M.; Greaves, G.N.; Ryan, A.J.; Heeley, E. *J. Appl. Crystallogr.* **2003**, *36*, 791–794.
[55] Petukhov, A.V.; Thijssen, J.H.J.; 't Hart, D.C.; Imhof, A.; van Blaaderen, A.; Dolbnya, I.P.; Snigirev, A.; Moussaid, A.; Snigireva, I. *J. Appl. Crystallogr.* **2006**, *39*, 137–144.
[56] Narayanan, T.; Diat, O.; Bösecke, P. *Nucl. Instrum. Methods Phys. Res., Sect. A* **2001**, *467–468* (Part 2), 1005–1009.
[57] van den Pol, E.; Thies-Weesie, D.M.E.; Petukhov, A.V.; Vroege, G.J.; Kvashnina, K. *J. Chem. Phys.* **2008**, *129* (16), 164715.
[58] Bolhuis, P.G.; Kofke, D.A. *Phys. Rev. E: Stat., Nonlinear, Soft Matter Phys.* **1996**, *54* (1), 634.
[59] Bartlett, P.; Warren, P.B. *Phys. Rev. Lett.* **1999**, *82* (9), 1979.
[60] Bates, M.A.; Frenkel, D. *J. Chem. Phys.* **1998**, *109* (14), 6193–6199.
[61] Fraden, S.; Hurd, A.J.; Meyer, R.B.; Cahoon, M.; Caspar, D.L.D. *J. Phys. Colloq.* **1985**, *46* (C3), 85–113.
[62] de Gennes, P.G.; Prost, J. *The Physics Of Liquid Crystals*; Clarendon: Oxford, 1995.
[63] Lemaire, B.J.; Davidson, P.; Petermann, D.; Panine, P.; Dozov, I.; Stoenescu, D.; Jolivet, J.P. *Eur. Phys. J. E* **2004**, *13*, 309–319.
[64] van den Pol, E.; Thies-Weesie, D.M.E.; Petukhov, A.V.; Panine, P.; Vroege, G.J. *J. Phys. Condens. Matter* **2008**, *20*, 404219.
[65] Lekkerkerker, H.N.W.; Coulon, P.; Van Der Haegen, R.; Deblieck, R. *J. Chem. Phys.* **1984**, *80* (7), 3427–3433.
[66] Speranza, A.; Sollich, P. *J. Chem. Phys.* **2002**, *117* (11), 5421–5436.
[67] Wensink, H.H.; Vroege, G.J. *J. Chem. Phys.* **2003**, *119* (13), 6868–6882.